

University of Nebraska - Lincoln

## DigitalCommons@University of Nebraska - Lincoln

---

Faculty Publications from the Department of  
Electrical and Computer Engineering

Electrical & Computer Engineering, Department  
of

---

12-16-2013

### Multiplexed fiber-ring laser sensors for ultrasonic detection

Tongqing Liu

*University of Nebraska-Lincoln*

Lingling Hu

*University of Nebraska-Lincoln*

Ming Han

*University of Nebraska-Lincoln*, [mhan@egr.msu.edu](mailto:mhan@egr.msu.edu)

Follow this and additional works at: <https://digitalcommons.unl.edu/electricalengineeringfacpub>



Part of the [Computer Engineering Commons](#), and the [Electrical and Computer Engineering Commons](#)

---

Liu, Tongqing; Hu, Lingling; and Han, Ming, "Multiplexed fiber-ring laser sensors for ultrasonic detection" (2013). *Faculty Publications from the Department of Electrical and Computer Engineering*. 235.  
<https://digitalcommons.unl.edu/electricalengineeringfacpub/235>

This Article is brought to you for free and open access by the Electrical & Computer Engineering, Department of at DigitalCommons@University of Nebraska - Lincoln. It has been accepted for inclusion in Faculty Publications from the Department of Electrical and Computer Engineering by an authorized administrator of DigitalCommons@University of Nebraska - Lincoln.

# Multiplexed fiber-ring laser sensors for ultrasonic detection

Tongqing Liu, Lingling Hu, and Ming Han\*

Department of Electrical Engineering, University of Nebraska-Lincoln, Lincoln, Nebraska, 68588, USA  
\*mhan3@unl.edu

**Abstract:** We propose and demonstrate a multiplexing method for ultrasonic sensors based on fiber Bragg gratings (FBGs) that are included inside the laser cavity of a fiber-ring laser. The multiplexing is achieved using add-drop filters to route the light signals, according to their wavelengths, into different optical paths, each of which contains a separate span of erbium-doped fiber (EDF) as the gain medium. Because a specific span of EDF only addresses a single wavelength channel, mode completion is avoided and the FBG ultrasonic sensors can be simultaneously demodulated. The proposed method is experimentally demonstrated using a two-channel system with two sensing FBGs in a single span of fiber.

©2013 Optical Society of America

**OCIS codes:** (060.2370) Fiber optics sensors; (060.3735) Fiber Bragg gratings; (060.3510) Lasers, fiber; (120.4290) Nondestructive testing.

---

## References and links

1. I. M. Perez, H. L. Cui, and E. Udd, "Acoustic emission detection using fiber Bragg gratings," *Proc. SPIE* **4328**, 209–215 (2001).
2. Y. Qiao, Y. Zhou, and S. Krishnaswamy, "Adaptive demodulation of dynamic signals from fiber Bragg gratings using two-wave mixing technology," *Appl. Opt.* **45**(21), 5132–5142 (2006).
3. D. Gatti, G. Galzerano, D. Janner, S. Longhi, and P. Laporta, "Fiber strain sensor based on a pi-phase-shifted Bragg grating and the Pound-Drever-Hall technique," *Opt. Express* **16**(3), 1945–1950 (2008).
4. A. Rosenthal, D. Razansky, and V. Ntziachristos, "High-sensitivity compact ultrasonic detector based on a pi-phase-shifted fiber Bragg grating," *Opt. Lett.* **36**(10), 1833–1835 (2011).
5. P. Fomitchov and S. Krishnaswamy, "Response of a fiber Bragg grating ultrasonic sensor," *Opt. Eng.* **42**(4), 956–963 (2003).
6. Q. Wu and Y. Okabe, "High-sensitivity ultrasonic phase-shifted fiber Bragg grating balanced sensing system," *Opt. Express* **20**(27), 28353–28362 (2012).
7. T. Q. Liu and M. Han, "Analysis of  $\pi$ -phase-shifted fiber Bragg gratings for ultrasonic detection," *IEEE Sens. J.* **12**(7), 2368–2373 (2012).
8. M. Han, T. Q. Liu, L. L. Hu, and Q. Zhang, "Intensity-demodulated fiber-ring laser sensor system for acoustic emission detection," *Opt. Express* **21**(24), 29269–29276 (2013).
9. M. A. Mirza and G. Stewart, "Multiwavelength operation of erbium-doped fiber lasers by periodic filtering and phase modulation," *J. Lightwave Technol.* **27**(8), 1034–1044 (2009).
10. N. Park and P. F. Wysocki, "24-line multiwavelength operation of erbium-doped fiber-ring laser," *Ieee Photonic Technol. Lett.* **8**(11), 1459–1461 (1996).
11. J. J. Tian, Y. Yao, Y. X. Sun, X. L. Yu, and D. Y. Chen, "Multiwavelength Erbium-doped fiber laser employing nonlinear polarization rotation in a symmetric nonlinear optical loop mirror," *Opt. Express* **17**(17), 15160–15166 (2009).
12. M. Zhou, Z. Q. Luo, J. Z. Wang, C. C. Ye, H. Y. Fu, C. Zhang, Z. P. Cai, and H. Y. Xu, "Graphene-assisted all-fiber multiwavelength erbium-doped fiber laser functionalized with evanescent field interaction," *Laser Phys.* **22**(5), 991–995 (2012).
13. T. Erdogan, "Fiber grating spectra," *J. Lightwave Technol.* **15**(8), 1277–1294 (1997).
14. G. A. Cranch, M. A. Englund, and C. K. Kirkendall, "Intensity noise characteristics of erbium-doped distributed-feedback fiber lasers," *IEEE J. Quantum Electron.* **39**(12), 1579–1586 (2003).
15. J. L. Rose, *Ultrasonic Waves in Solid Media* (Cambridge University Press, 1999).

---

## 1. Introduction

Fiber-optic ultrasonic sensors based on regular fiber Bragg gratings (FBGs) or  $\pi$ -phase-shifted FBGs have received a great deal of attention in the past decades for their potential applications in structural health monitoring such as ultrasonic testing and acoustic emission (AE) detection [1–7]. A common demodulation method for these sensors is to use a tunable

laser whose wavelength is set within a linear range of the grating spectrum. The ultrasonic signal is detected by monitoring the laser intensity variations caused by the ultrasound-induced spectral shift of the grating spectrum. In many applications, such as the AE detection of air-craft structure during operation, the FBG may experience large quasi-static strains, which imposes demanding requirement on the speed and wavelength range of the tunable laser source. The low-cost temperature- or current-tuned diode lasers are not sufficient and more sophisticated tunable lasers such as the external cavity lasers with piezoelectric tuning capability have to be used. Because a FBG only occupies a small spectral bandwidth, a prominent advantage of FBG-based fiber-optic sensors is that many sensors can be multiplexed in a single span of fiber and the signals from the sensors are separated in the wavelength domain. However, due to the high cost of tunable lasers, multiplexed ultrasound detection based on FBGs, in which each sensor requires a tunable laser at a unique wavelength, has rarely been demonstrated and may not be practically feasible. Recently, we have proposed and demonstrated a potentially low-cost fiber-optic ultrasonic sensor system for acoustic emission detection by incorporating a narrow-band tunable optical band-pass filter (TOBPF) and a sensing FBG inside the laser cavity of a fiber-ring laser (FRL) that employs an erbium-doped fiber (EDF) as the gain medium [8]. The sensor system has a simple structure and its operation does not require external tunable lasers. However, employing such a method for multiplexed FBG ultrasonic sensors is not straight-forward. The EDF is homogeneously broadened at room temperature, leading to mode competition and potential instable lasing operation if multiple FBGs are included in the same FRL cavity. Although many techniques have been studied and demonstrated to suppress the mode competition in a FRL in the context of developing multi-wavelength laser sources used for optical communications [9–12], these techniques cannot be applied for FRLs used as ultrasonic sensors.

In this paper, we propose a novel FRL sensor system which can demodulate multiple FBG ultrasonic sensors multiplexed on a single-span of fiber. It is based on add-drop filters through which each FBG is involved in an optical path with a unique span of EDF so that mode competition is avoided. The proposed multiplexed sensor system also has a simple structure and only uses standard fiber-optic components. Each channel of the multiplexed system detects the ultrasonic signal using the same principle as in a single-point FRL sensor system demonstrated in [8]. The sensors are demodulated directly from the variations of the laser output power by a photodetector (PD). Therefore, the proposed system is potentially low cost.

## 2. Principle of operation

The schematic of the proposed multiplexed FRL ultrasonic sensor system is shown in Fig. 1(a). It can be divided into two parts that are connected by an optical fiber: the sensors and the demodulation box. The sensors are a number of FBGs multiplexed on a single span of fiber, each of which has a different Bragg wavelength so that their reflection spectra are separated in the wavelength domain. The demodulation box consists of a number of add-drop filters formed by FBGs and fiber-optic circulators. Each of the add-drop filters corresponds to a FBG wavelength channel. The light reflected from a FBG is dropped from the “main loop” by the corresponding add-drop filter, which is subsequently amplified by the EDF pumped by a pump laser (not shown here) and then added to the main loop again by the same add-drop filter. To further explain its principle of operation, Fig. 1(b) shows the optical paths in the demodulation box for three FBG channels. Using the channel of wavelength  $\lambda_2$  as an example, the light at  $\lambda_2$  from the main loop passes through circulator C1, then through FBG1 that has a different wavelength of  $\lambda_1$ , and finally through circulator C2a before it is reflected back to C2a by FBG2a that is designed to reflect light with a wavelength around  $\lambda_2$ . The reflected light is then “dropped” to the channel containing EDF2 by circulator C2a and is amplified by the EDF. The amplified light then passes through circulator C2b and is reflected back to C2b by FBG2b that has identical reflection properties to FBG2a. The reflected light is guided to port 3 of circulator C2b and passes through FBG3b and C3b to be “added” back to the main

loop. It is seen that, although the FBGs are connected in series in a fiber, their common optical path does not contain any EDF and each FBG is involved in a unique FRL cavity loop using a unique EDF as the gain medium. Therefore, there is no mode competition and the lasing is stable.

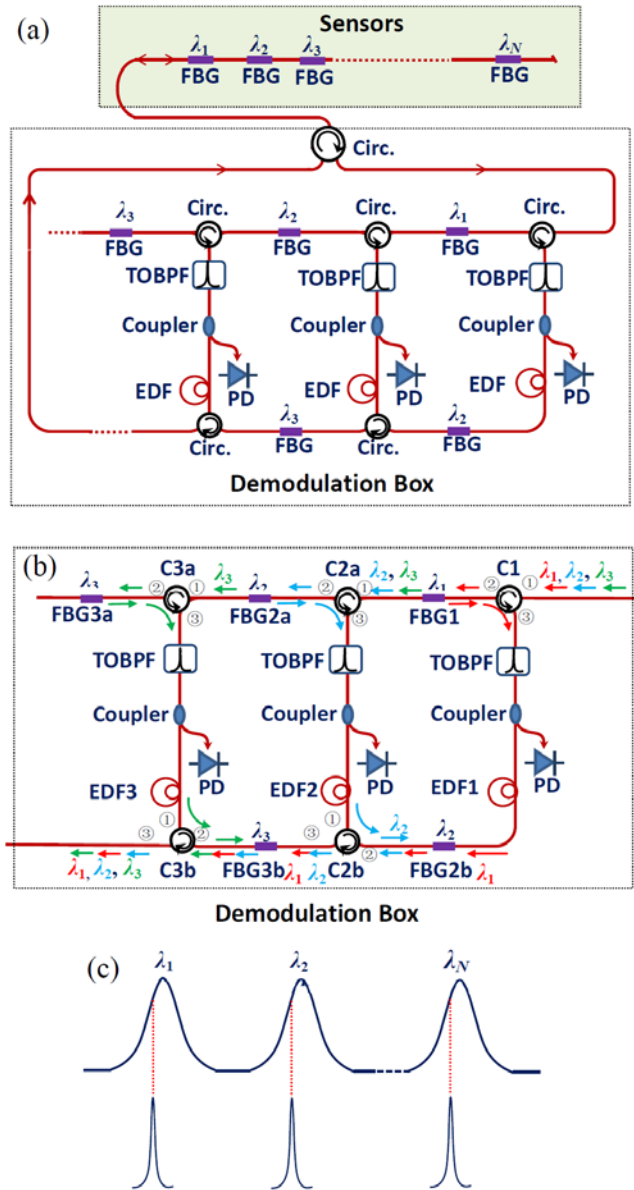


Fig. 1. Schematic of (a) the proposed multiplexed FRL ultrasonic sensor system, (b) the optical pathways of light in the demodulation box, and (c) the reflection spectrum of the sensing FBGs and the transmission spectrum of the TOBPFs. Circ.: circulator

For each channel, the principle for the ultrasonic detection is the same as described in [8]. More specifically, as shown in Fig. 1(c), a narrow TOBPF is included before the EDF for each channel. The transmission peak of the TOBPF is much narrower than the reflection bandwidth of the corresponding FBG so that the fiber laser wavelength is determined by the TOBPF. To perform ultrasonic detection, the center wavelength of the TOBPF is tuned on a

spectral slope of the FBG. The ultrasonic signal that impinges onto the FBG causes the spectral shift of the FBG spectrum, which in turn modulates the cold cavity loss of this particular channel of the FRL. It has been theoretically and experimentally demonstrated that the FRL power fluctuates according to the loss modulation [8]. Therefore, the ultrasonic signal that impinges on a particular FBG can be detected from the variations of the laser output power of the corresponding FRL channel, which is monitored by a PD through a fiber-optic coupler.

Note that, to account for the potentially large spectral drift of the sensing FBG caused by temperature variations or other environmental and structural perturbations, the reflection spectra of the FBGs in the demodulation box need to be sufficiently broad so that no active tuning of the FBGs is required. Both short and strong regular FBGs and chirped FBGs [13], whose spectra can be designed to be flat and highly reflective in a relatively broad wavelength range, are excellent choices for these FBGs.

### 3. Experiment

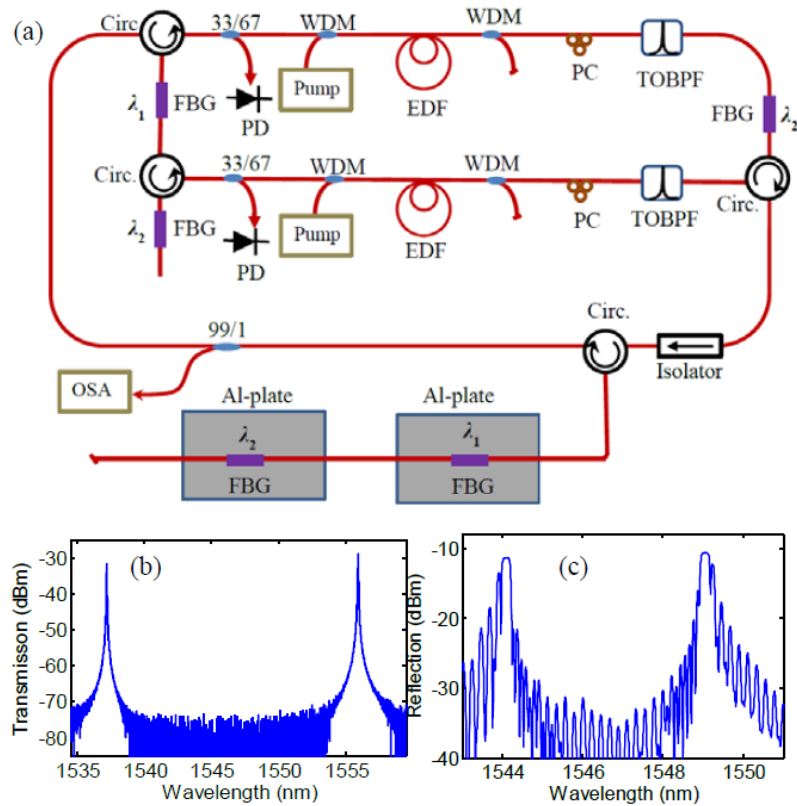


Fig. 2. (a) Schematic of the experimental setup; (b) measured transmission spectrum of one of the two TOBPF; and (c) measured reflection spectrum of the two cascaded sensing FBGs.

The proposed multiplexing method was experimentally demonstrated for a two-channel sensor system using a setup schematically shown in Fig. 2(a). For each channel, the cavity length of the FRL channel was estimated to be  $\sim 20$  m and the gain medium was a 3-m long EDF (Model: I-6, Fibertec, UK) pumped by a 980 nm diode laser through a 980/1550 wavelength-division multiplexer (WDM). An additional 980/1550 nm WDM was included in each channel to guide the residual pump power out of the laser cavity. A fiber-optic coupler was used before each of the WDMs to couple 33% of the laser power of that particular channel out of the laser cavity that was detected by a PD. The TOBPFs (Model: FFP-TF2,

Micron Optics) are based on high-finesse Fabry-Perot interferometers and they were electronically tuned by a two-channel dc voltage source. Both of the TOBPFs have similar parameters: free-spectral range of ~18 nm, 3-dB bandwidth of ~26 pm, and insertion loss at the transmission peaks of ~3 dB. Figure 2(b) shows the transmission spectrum of one of the TOBPFs measured by an optical spectrum analyzer (OSA) (Model: AQ6370C, Yokogawa) using a broadband light source. The FRL main loop contained a 99/1 fiber-optic coupler to couple out 1% of the light power for the monitoring of the optical spectrum in the main loop using an OSA. The two sensing FBGs were ~7 mm long and fabricated directly onto a regular SMF using a phase mask and a 193 nm excimer laser. Their Bragg wavelengths are around 1549 nm for Channel 1 ( $\lambda_1$ ) and around 1544 nm for Channel 2 ( $\lambda_2$ ), as shown by their reflection spectra in Fig. 2(c) measured by a sensor interrogator (Model: sm125, Micron Optics). Each of the sensing FBGs was bonded on a separate 2' × 2' aluminum (Al)-plate using a general-purpose adhesive. The FBGs for each of the two channels in the demodulation box were fabricated using the same fabrication setup for the sensing FBGs. Their reflectivity at the Bragg wavelength is >99.9% as estimated by their transmission spectra measured by the OSA and their wavelengths match the wavelengths of the corresponding sensing FBGs.

The generation of the testing ultrasonic signal, the reference sensor for comparison, and the processing of the signal from the PDs are similar to those used in [8] and not shown in Fig. 1(a). Specifically, the ultrasonic signal was generated by a piezoelectric transducer (PZT) (Model: HD50, Physical Acoustic Corporation) that was placed on the top surface of the Al-plate. Another PZT sensor (Model: R15 $\alpha$ , Physical Acoustic Corporation) was placed near the sensing FBG and was used as the reference sensor for comparison with the FRL sensor system. Liquid ultrasonic couplant was applied between the Al-plates and the PZTs to improve the ultrasonic coupling efficiency. The signals from the PDs were amplified by an amplifier with a built-in band-pass filter from 20 kHz to 1.2 MHz followed by a 150 kHz electrical high-pass filter.

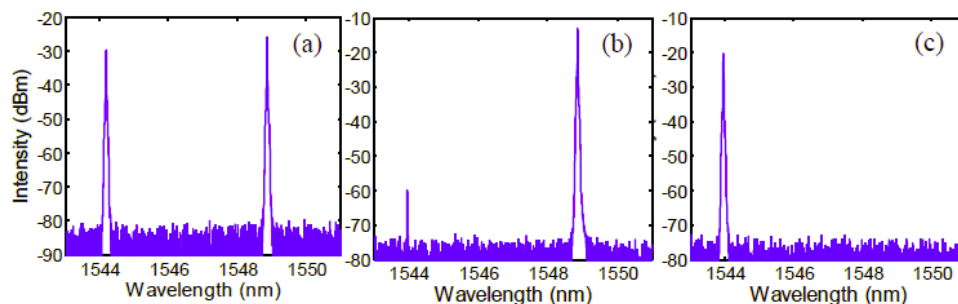


Fig. 3. Optical spectra measured by the OSA at the output from (a) the 99/1 fiber coupler; (b) the 67/33 fiber coupler in Channel 1; and (c) the 67/33 fiber coupler in Channel 2.

The TOBPFs were tuned to the positions where the FRL can simultaneously lase at the two channel wavelengths. Note that the dc supply that was used to tune the TOBPFs was not optimized for the application and its output voltage exhibited relatively large low-frequency drift. As a result, the voltages need to be adjusted intermittently for sustained lasing. Figure 3(a) shows a typical optical spectrum in the main loop of the FRL measured by an OSA through the 99/1 coupler shown in Fig. 2(a). The peaks at the two wavelengths (~1544 and ~1549 nm) clearly indicate that the sensor system lases simultaneously for both channels corresponding to the Bragg wavelengths of the two sensing FBGs. Figure 3(b) is a typical optical spectrum measured for the optical signal from Channel 1 through the 33/67 fiber coupler as in Fig. 2(a). In addition to the main peak corresponding to the channel wavelength, a small peak corresponding to the wavelength of Channel 2 is also present, indicating that some of laser energy in Channel 2 leaked into Channel 1, possibly due to the small reflection from the spectral sidelopes of the FBG ( $\lambda_1$ ) in Channel 1. However, the leaked energy is about

50 dB below the main peak. Such a low-level leakage can be ignored in most cases and should not cause cross-channel interference for ultrasonic detection. Figure 3(c) is the spectrum of the optical signal from Channel 2 measured through the 33/67 fiber coupler in that channel. In this case, only one peak corresponding to the channel wavelength is present.

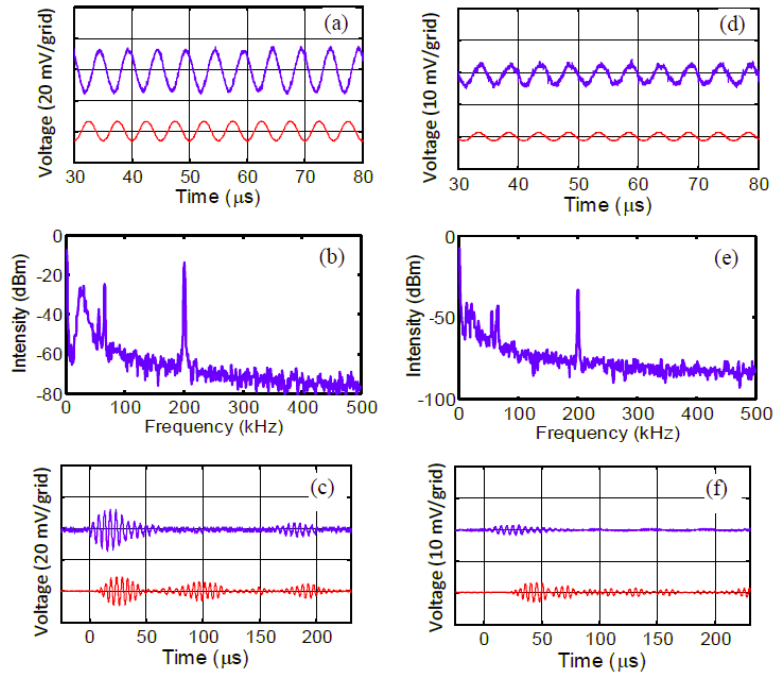


Fig. 4. Experimental results. (a) and (c): Responses of PZT and FRL sensors to continuous ultrasonic waves; (b) and (d): electrical spectra measured by the SA; (e) and (f): responses of PZT and FRL sensors to ultrasonic pulses. (a)-(c) are results for Channel 1 and (d)-(f) are for Channel 2. The FRL sensor response shown in (f) is an 8-time average measurement result.

The sensors were first tested for detection of continuous ultrasonic waves, which was generated by the PZT source powered by a continuous sinusoidal voltage signal with a frequency of 200 kHz and a peak-to-peak voltage of 20 V. The ultrasonic waves were separately applied on the two sensing FBGs. Figure 4(a) shows the responses from both the reference PZT sensor and the FRL sensor for Channel 1 when the TOBPF was tuned to the position where the sensor was most sensitive. Note that the signal from the PD for the FRL sensor was amplified and filtered as described above. The similarity between the signals from both the PZT and the FRL sensors clearly indicates that the FRL sensor can faithfully detect the ultrasonic signal. Figure 4(b) is the electrical spectrum of the signal before the 150 kHz high-pass filter measured by a spectrum analyzer (SA). The strong peak at 200 kHz corresponds to the response of the FRL sensor to the ultrasonic signal. The spectrum also shows several peaks at the lower frequency range between 20 and 70 kHz, corresponding to the relaxation oscillation of the FRL, which was also theoretically predicted and experimentally observed in a single-channel FRL sensor system reported earlier [8]. The relaxation oscillation is a result of the dynamic energy interchange process between the pump photons and the lasing photons through the gain medium [14]. To further verify the ultrasonic detection capability for this channel, the sensor was applied to ultrasonic pulses generated from the same PZT source powered by a repeating 5-cycle 200 kHz sinusoidal voltage signal with peak-to-peak voltage of 20 V. The ultrasonic pulses propagate in the plate as Lamb waves of different modes [15]. Figure 4(c) shows the responses from the FRL sensor and the PZT sensor, which agree well with each other considering that the PZT sensor and the FBG may respond differently to different Lamb modes.

The above ultrasonic testing parameters and processes for Channel 1 were repeated for Channel 2 and the results are shown in Figs. 4(d)-4(f). These results are similar to those obtained for Channel 1. The results for both channels are also similar to the results of a single-channel system described in [8]. In addition, we observed no cross-channel response for any of the two channels. Therefore we conclude that the channels in this multiplexing system work independently for ultrasonic detection. Note that the signals from Channel 2 are weaker than that from Channel 1 for both the continuous ultrasonic wave testing and the ultrasonic pulse testing. It is mainly due to the weaker ultrasonic signal for Channel 2, as evidenced by weaker signals from the reference PZT sensor shown in Fig. 4. We noticed that the Al-plate for Channel 2 was slightly bent which may lead to reduced ultrasonic coupling efficiency from the PZT source to the Al-plate for the channel. The slight differences in the shapes of the PZT sensor signals for the two channels may arise from the structural differences (such as thickness and deformations) of the two Al plates, leading to different distributions of the ultrasonic energy among the Lamb modes, and the different relative positions of the PZT source and the PZT sensor installed on the two Al plates.

It is worth noting that the lasing output for each channel contains a large number of densely-spaced longitudinal modes due to the long laser cavity length for each FRL channel (~20 m). However, we did not observe significant noises specific to the mode competition and mode hopping during the detection of the ultrasonic signals, which is reasonable because the mode hopping and mode completion occurs randomly among a large number of these longitudinal modes and the noise generated by these events partially cancel out each other.

#### **4. Summary**

We have proposed and experimentally demonstrated a novel multiplexing methodology for ultrasonic sensors based on FBGs that are included in the laser cavity of a FRL system. Through add-drop filters, the lasers corresponding to different channels from the common path are routed into different paths each of which has a separate span of EDF. As a result, the mode completion is avoided; stable lasing is achieved for all channels. We have constructed a two-channel system and each of the channels was demonstrated to successfully detect ultrasonic signals generated from a PZT source. Although we only experimentally demonstrated a two-channel system, the capacity can be easily expanded by adding more channel modules to the existing system. Such a multiplexed fiber-optic ultrasonic sensor system may be used for acoustic emission detection for structural health monitoring.

#### **Acknowledgments**

This work was supported by the Office of Naval Research under grants N000141310159 and N000141110262, and the National Science Foundation under grant EPS-1004094.